PROCEEDINGS OF SCIENCE

Test of QCD at large Q^2 with exclusive hadronic processes

Chengping Shen[*†]
School of Physics and Nuclear Energy Engineering, Beihang University, Beijing, 100191, China
E-mail: shencp@ihep.ac.cn

(1). Using samples of 102 million $\Upsilon(1S)$ and 158 million $\Upsilon(2S)$ events at Belle, we study 17 exclusive hadronic decay modes of these two bottomonium resonances to some Vector-Pseudoscalar (VP), Vector-Tensor (VT) and Axial-vector-Pseudoscalar (AP) processes and their final states. Branching fractions are measured for all the processes. The ratios of the branching fractions of $\Upsilon(2S)$ and $\Upsilon(1S)$ decays into the same final state are used to test a perturbative QCD (pQCD) prediction for OZI-suppressed bottomonium decays. (2). Using data samples of 89 fb^{-1}, 703 fb^{-1}, and 121 fb^{-1} collected at center-of-mass (CMS) energies 10.52, 10.58, and 10.876 GeV, respectively, we measure the cross sections of $e^+e^- \to \omega\pi^0$, $K^*(892)\bar{K}$, and $K_2^*(1430)\bar{K}$. The energy dependence of the cross sections is presented.

XV International Conference on Hadron Spectroscopy-Hadron 2013
4-8 November 2013
Nara, Japan

[*]Speaker.

[†]On behalf of the Belle Collaboration and supported partly by the Fundamental Research Funds for the Central Universities of China (303236).

PoS(Hadron 2013)132

1. Measurements of $\Upsilon(1S)$ and $\Upsilon(2S)$ decays into VT, AP and VP final states

For the OZI (Okubo-Zweig-Iizuka) suppressed decays of the J/ψ and $\psi(2S)$ to hadrons, pQCD provides a relation for the ratios of branching fractions ($\mathscr{B}$) for J/ψ and $\psi(2S)$ decays

$$Q_\psi = \frac{\mathscr{B}_{\psi(2S)\to\text{hadrons}}}{\mathscr{B}_{J/\psi\to\text{hadrons}}} = \frac{\mathscr{B}_{\psi(2S)\to e^+e^-}}{\mathscr{B}_{J/\psi\to e^+e^-}} \approx 12\%, \tag{1.1}$$

which is referred to as the "12% rule" [1]. However, it is found to be severely violated for $\rho\pi$ and other VP and VT final states. A similar rule can be derived for OZI-suppressed bottomonium decays:

$$Q_\Upsilon = \frac{\mathscr{B}_{\Upsilon(2S)\to\text{hadrons}}}{\mathscr{B}_{\Upsilon(1S)\to\text{hadrons}}} = \frac{\mathscr{B}_{\Upsilon(2S)\to e^+e^-}}{\mathscr{B}_{\Upsilon(1S)\to e^+e^-}} = 0.77 \pm 0.07. \tag{1.2}$$

Using 102 million $\Upsilon(1S)$ events, 158 million $\Upsilon(2S)$ events, and a 89.4 fb^{-1} continuum data sample at $\sqrt{s} = 10.52$ GeV, Belle has studied some exclusive decay channels to test such rule [2].

Figure 1 shows the $K^+\pi^-$ invariant-mass distribution from $\Upsilon(1S) \to K^+K^-\pi^+\pi^-$ and also shows the mass projections for the vector $K^{*0}(892)$ and tensor meson $\bar{K}_2^{*0}(1430)$ candidates from 2D fits to the events from $\Upsilon(1S) \to K^{*0}(892)\bar{K}_2^{*0}(1430)$ decay. Clear signals could be observed. For the details to the other three-body ϕK^+K^-, $\omega\pi^+\pi^-$, and $K^{*0}(892)K^-\pi^+$ and two-body VT ($\phi f_2'(1525)$, $\omega f_2(1270)$, $\rho a_2(1320)$, and $K^{*0}(892)\bar{K}_2^{*0}(1430)$) and AP ($K_1(1270)^+K^-$, $K_1(1400)^+K^-$, and $b_1(1235)^+\pi^-$) final states from $\Upsilon(1S)$ and $\Upsilon(2S)$ decays, please refer to Ref. [3].

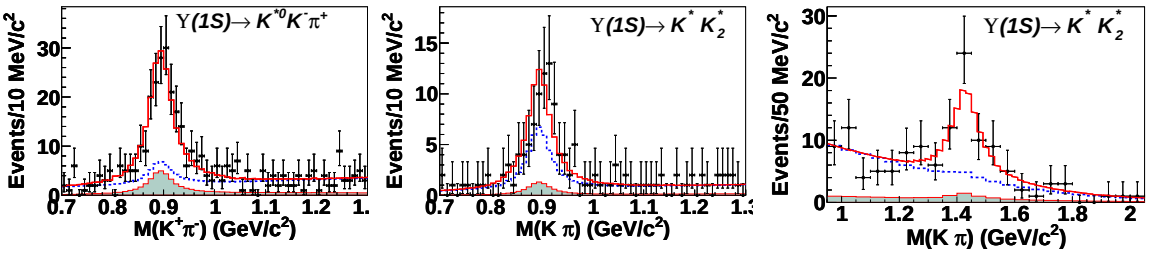

Figure 1: The $K^+\pi^-$ (left panel) invariant-mass distribution for the final candidate events from $\Upsilon(1S) \to K^+K^-\pi^+\pi^-$. And the mass projections for the vector $K^{*0}(892)$ (middle panel) and tensor meson $\bar{K}_2^{*0}(1430)$ (right panel) candidates from 2D fits to the events from $\Upsilon(1S)$ two-body decay. The open histograms show the results, the dotted curves show the total background estimates, and the shaded histograms are the normalized continuum contributions.

Figure 2 shows the scaled total energy $X_T = \sum_h E_h/\sqrt{s}$ distribution, where E_h is the energy of the final-state particle h in the e^+e^- CMS frame, and the $K^+\pi^-$, $K_S^0\pi^-$ mass distributions for the $K^*(892)^0$, $K^*(892)^-$ vector meson candidates from $\Upsilon(1S) \to K_S^0K^+\pi^-$ decay together with the fitted results. Clear $K^{*0}(892)$ signal is observed. For the details to the other $K_S^0K^+\pi^-$, $\pi^+\pi^-\pi^0\pi^0$, and $\pi^+\pi^-\pi^0$, and two-body VP ($K^*(892)^0\bar{K}^0$, $K^*(892)^-K^+$, $\omega\pi^0$, and $\rho\pi$) final states from $\Upsilon(1S)$ and $\Upsilon(2S)$ decays, please refer to Ref. [4].

Table 1 gives the final results for the $\Upsilon(1S)$ and $\Upsilon(2S)$ decays branching fractions and the calculated corresponding ratio for all the modes. Form these results, we see for $\omega\pi^+\pi^-$, $\pi^+\pi^-\pi^0$ and $b_1(1235)^+\pi^-$ the Q_Υ ratio is a little lower than the pQCD prediction. The results for the other modes are inconclusive due to low statistical significance. These results may supply useful

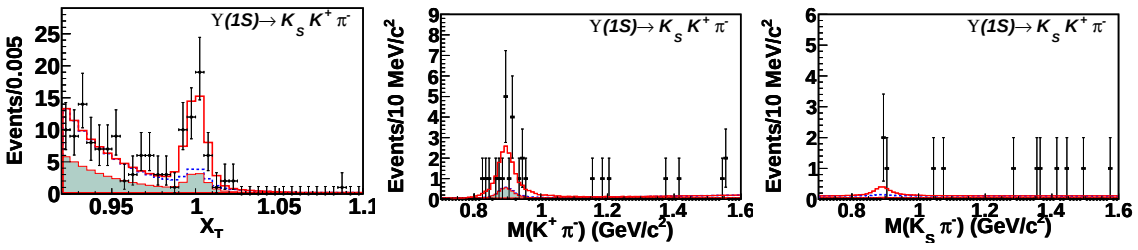

Figure 2: The fit to the scaled total energy X_T distribution (left panel) and the fits to the $K^+\pi^-$, $K^0_S\pi^-$ mass distributions (middle and right panels) for the $K^*(892)^0$, $K^*(892)^-$ vector meson candidates from $\Upsilon(1S) \to K^0_S K^+\pi^-$ decay. The solid histograms show the best fits, dashed curves are the total background estimates, and shaded histograms are the normalized continuum background contributions.

Table 1: Results for the $\Upsilon(1S)$ and $\Upsilon(2S)$ decays, where $\mathscr{B}$ is the branching fraction, $\mathscr{B}^{\rm UP}$ is the upper limit on the branching fraction, Q_Υ is the ratio of the $\Upsilon(2S)$ and $\Upsilon(1S)$ branching fractions, and $Q^{\rm UP}_\Upsilon$ is the upper limit on the value of Q_Υ. Branching fractions are in units of 10^{-6} and upper limits are given at the 90% C.L. The first error in $\mathscr{B}$ and Q_Υ is statistical, and the second is systematic.

Mode	Channel	$\Upsilon(1S)$		$\Upsilon(2S)$			
		$\mathscr{B}$	$\mathscr{B}^{\rm UP}$	$\mathscr{B}$	$\mathscr{B}^{\rm UP}$	Q_Υ	$Q^{\rm UP}_\Upsilon$
3- or 4-body processes	ϕK^+K^-	$2.36\pm0.37\pm0.29$	—	$1.58\pm0.33\pm0.18$	—	$0.67\pm0.18\pm0.11$	—
	$\omega\pi^+\pi^-$	$4.46\pm0.67\pm0.72$	—	$1.32\pm0.54\pm0.45$	2.58	$0.30\pm0.13\pm0.11$	0.55
	$K^{*0}K^-\pi^+$	$4.42\pm0.50\pm0.58$	—	$2.32\pm0.40\pm0.54$	—	$0.52\pm0.11\pm0.14$	—
	$K^0_SK^+\pi^-$	$1.59\pm0.33\pm0.18$	—	$1.14\pm0.30\pm0.13$	—	$0.72\pm0.24\pm0.09$	—
	$\pi^+\pi^-\pi^0\pi^0$	$12.8\pm2.01\pm2.27$	—	$13.0\pm1.86\pm2.08$	—	$1.01\pm0.22\pm0.23$	—
	$\pi^+\pi^-\pi^0$	$2.14\pm0.72\pm0.34$	—	$-0.10\pm0.46\pm0.02$	0.80	$-0.05\pm0.21\pm0.02$	0.42
VT	$\phi f_2'$	$0.64\pm0.37\pm0.14$	1.63	$0.50\pm0.36\pm0.19$	1.33	$0.77\pm0.70\pm0.33$	2.54
	ωf_2	$0.57\pm0.44\pm0.13$	1.79	$-0.03\pm0.24\pm0.01$	0.57	$-0.06\pm0.42\pm0.02$	1.22
	ρa_2	$1.15\pm0.47\pm0.18$	2.24	$0.27\pm0.28\pm0.14$	0.88	$0.23\pm0.26\pm0.12$	0.82
	$K^{*0}\bar{K}^{*0}_2$	$3.02\pm0.68\pm0.34$	—	$1.53\pm0.52\pm0.19$	—	$0.50\pm0.21\pm0.07$	—
AP	$K_1(1270)^+K^-$	$0.54\pm0.72\pm0.21$	2.41	$1.06\pm0.42\pm0.32$	3.22	$1.96\pm2.71\pm0.84$	4.73
	$K_1(1400)^+K^-$	$1.02\pm0.35\pm0.22$	—	$0.26\pm0.23\pm0.09$	0.83	$0.26\pm0.25\pm0.10$	0.77
	$b_1(1235)^+\pi^-$	$0.47\pm0.22\pm0.13$	1.25	$0.02\pm0.07\pm0.01$	0.40	$0.05\pm0.16\pm0.03$	0.35
VP	$K^*(892)^0\bar{K}^0$	$2.92\pm0.85\pm0.37$	—	$1.79\pm0.73\pm0.30$	4.22	$0.61\pm0.31\pm0.12$	1.20
	$K^*(892)^-K^+$	$0.31\pm0.30\pm0.04$	1.11	$0.58\pm0.35\pm0.09$	1.45	$1.87\pm2.12\pm0.33$	5.52
	$\omega\pi^0$	$1.32\pm1.11\pm0.14$	3.90	$0.03\pm0.68\pm0.01$	1.63	$0.02\pm0.50\pm0.01$	1.68
	$\rho\pi$	$1.75\pm0.91\pm0.28$	3.68	$-0.11\pm0.64\pm0.03$	1.16	$-0.06\pm0.38\pm0.02$	0.94

guidance for interpreting violations of the 12% rule for OZI suppressed decays in the charmonium sector.

2. Measurement of $e^+e^- \to \omega\pi^0$, $K^*(892)\bar{K}$ and $K^*_2(1430)\bar{K}$ at $\sqrt{s}$ near 10.6 GeV

The energy dependence of the cross sections for $e^+e^- \to$ VP is different under different theoretical models. We have the cross sections ratio relation $\omega\pi^0 : K^*(892)^0\bar{K}^0 : K^*(892)^-K^+ = 9:8:2$ with $SU(3)_f$ symmetry. But with the CLEO experiment measurement at $\sqrt{s} = 3.67$ GeV and 3.773 GeV [5], $R_{\rm VP} = \frac{\sigma_B(e^+e^-\to K^*(892)^0\bar{K}^0)}{\sigma_B(e^+e^-\to K^*(892)^-K^+)}$ is greater than 9 and 33 at $\sqrt{s} = 3.67$ GeV and 3.773 GeV, respectively, at the 90% C.L. By taking into account $SU(3)_{\rm f}$ symmetry break-

ing, a pQCD calculation predicts $R_{\rm VP} = 6.0$ [6]. In the quark model, one may naively expect $R_{\rm TP} = \frac{\sigma_B(e^+e^-\to K_2^*(1430)^0\bar{K}^0)}{\sigma_B(e^+e^-\to K_2^*(1430)^-K^+)} = R_{\rm VP}$.

After all the selection requirements, clear $e^+e^- \to \pi^+\pi^-\pi^0\pi^0$ and $K_S^0K^+\pi^-$ signals are observed in the X_T distributions, where E_h is the energy of the final-state particle h in the e^+e^- CMS frame. We require $|X_T - 1| < 0.025$ for $\pi^+\pi^-\pi^0\pi^0$ and $|X_T - 1| < 0.02$ for $K_S^0K^+\pi^-$ to select signal candidates. For the selected events, Fig. 3 shows the $\pi^+\pi^-\pi^0$, $K^+\pi^-$, and $K_S^0\pi^-$ invariant mass distributions for the $\pi^+\pi^-\pi^0\pi^0$ and $K_S^0K^+\pi^-$ final states from the $\sqrt{s} = 10.58$ GeV data sample. The dots with error bars are from the data and the light shaded histograms are from the normalized $e^+e^- \to u\bar{u}/d\bar{d}/s\bar{s}$ backgrounds. In the $\pi^+\pi^-\pi^0$ invariant mass distributions, the dark shaded histograms in the ω and ϕ mass regions are from the normalized $e^+e^- \to \gamma_{\rm ISR}\omega/\phi \to \gamma_{\rm ISR}\pi^+\pi^-\pi^0$ backgrounds. In the $K^+\pi^-$ and $K_S^0\pi^-$ invariant mass distributions, we observe clear $K^*(892)^0$ and $K_2^*(1430)^-$ signals, while almost no signals for $K_2^*(1430)^0$ and $K^*(892)^-$ can be seen. The solid lines, shown in Fig. 3, are from unbinned maximum likelihood fits. For other plots from $\sqrt{s} = 10.52$ GeV and 10.876 GeV data samples, please refer to Ref. [7].

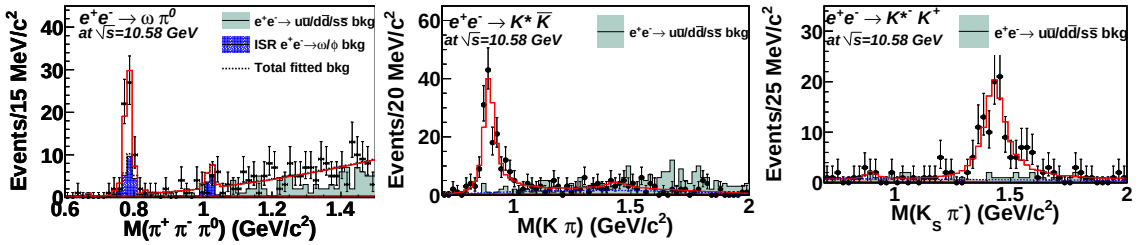

Figure 3: The fits to the $\pi^+\pi^-\pi^0$ (left), $K^+\pi^-$ (middle) and $K_S^0\pi^-$ (right) invariant mass distributions for the ω, $K^*(892)$, and $K_2^*(1430)$ meson candidates from $e^+e^- \to \pi^+\pi^-\pi^0\pi^0$ and $K_S^0K^+\pi^-$ events from the $\sqrt{s} = 10.58$ GeV data sample. The solid lines show the fit results, the dotted curves show the total background estimates, the dark shaded histograms are from the normalized ISR backgrounds $e^+e^- \to \gamma_{\rm ISR}\omega/\phi \to \gamma_{\rm ISR}\pi^+\pi^-\pi^0$ and the light shaded histograms are from the normalized $e^+e^- \to u\bar{u}/d\bar{d}/s\bar{s}$ backgrounds.

Table 2: Results for the Born cross sections, where σ_{Bi} ($i = 1,2,3$ for $\sqrt{s} = 10.52$, 10.58 and 10.876 GeV) is the Born cross section, $\sigma_{Bi}^{\rm UL}$ is the upper limit on the Born cross section. All the upper limits are given at the 90% C.L. The first uncertainty in σ_{Bi} is statistical, and the second is systematic.

Channel	σ_{B1} (fb) / $\sigma_{B1}^{\rm UL}$ (fb)	σ_{B2} (fb) / $\sigma_{B2}^{\rm UL}$ (fb)	σ_{B3} (fb) / $\sigma_{B3}^{\rm UL}$ (fb)
$\omega\pi^0$	$4.53^{+3.64}_{-2.88} \pm 0.50$ / 11	$6.01^{+1.29}_{-1.18} \pm 0.57$ / —	$-0.68^{+2.71}_{-1.97} \pm 0.20$ / 6.5
$K^*(892)^0\bar{K}^0$	$10.77^{+2.15}_{-1.90} \pm 0.77$ / —	$7.48 \pm 0.67 \pm 0.51$ / —	$7.58^{+1.64}_{-1.47} \pm 0.63$ / —
$K^*(892)^-K^+$	$1.14^{+0.90}_{-0.67} \pm 0.15$ / 2.3	$0.18^{+0.14}_{-0.12} \pm 0.02$ / 0.4	$0.28^{+0.68}_{-0.52} \pm 0.10$ / 1.5
$K_2^*(1430)^0\bar{K}^0$	$0.76^{+2.53}_{-2.26} \pm 0.14$ / 4.0	$1.65^{+0.86}_{-0.78} \pm 0.27$ / 3.1	$0.38^{+1.79}_{-1.47} \pm 0.07$ / 3.5
$K_2^*(1430)^-K^+$	$6.06^{+3.13}_{-2.93} \pm 1.34$ / 11	$8.36 \pm 0.95 \pm 0.62$ / —	$6.20^{+1.86}_{-1.63} \pm 0.64$ / —

Table 2 shows the results for the measured Born cross sections including the upper limits at 90% C.L. for the channels with a signal significance of less than 3σ. We fit the $1/s^n$ dependence of the cross sections for the processes $e^+e^- \to \omega\pi^0$ and $e^+e^- \to K^*(892)^0\bar{K}^0$ to our data and

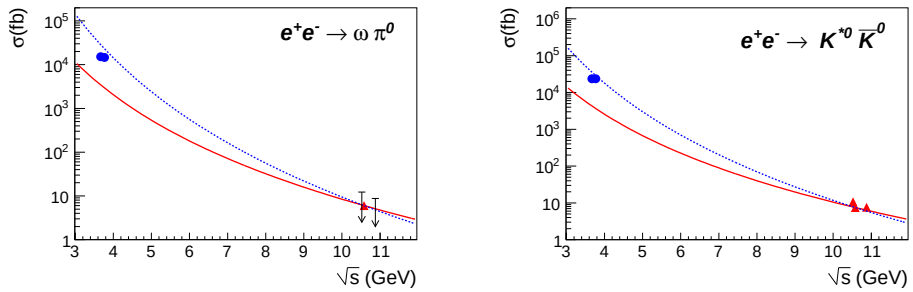

Figure 4: The cross sections for $e^+e^- \to \omega\pi^0$ and $K^*(892)^0\bar{K}^0$. The data at $\sqrt{s} = 10.52$, 10.58, and 10.876 GeV are from our measurements. The data at $\sqrt{s} = 3.67$ and 3.77 GeV are from CLEO measurement. Here, the uncertainties are the sum of the statistical and systematic uncertainties in quadrature. Upper limits are shown by the arrows. The solid line corresponds to a $1/s^3$ dependence and the dashed line to a $1/s^4$ dependence; the curves pass through the measured cross section at $\sqrt{s} = 10.58$ GeV.

those from CLEO at $\sqrt{s} = 3.67$ and 3.77 GeV [5]. The fit gives $n = 3.83 \pm 0.07$ and 3.75 ± 0.12 for $e^+e^- \to K^*(892)^0\bar{K}^0$ and $\omega\pi^0$, respectively. These differ significantly from the $1/s^2$ [8] or $1/s^3$ [6] predictions and agree with $1/s^4$ [9, 10, 11] within 2.5σ.

Based on the likelihood curves of the cross section measurements, in which the relevant systematic uncertainties are convolved, we obtain $R_{\rm VP} > 4.3, 20.0, 5.4$, and $R_{\rm TP} < 1.1, 0.4, 0.6$, for $\sqrt{s} = 10.52$, 10.58, and 10.876 GeV, respectively, at the 90% C.L. For $K^*(892)\bar{K}$, the ratio of the cross sections of $K^*(892)^0\bar{K}^0$ and $K^*(892)^-K^+$ at $\sqrt{s} = 10.58$ GeV is much larger than the predictions from exact or broken SU(3) symmetry models. Conversely, for $K_2^*(1430)\bar{K}$, the ratio of the cross sections of $K_2^*(1430)^0\bar{K}^0$ and $K_2^*(1430)^-K^+$ is much smaller than the prediction from the SU(3) symmetry or with the SU(3) symmetry breaking effects considered.

References

[1] T. Appelquist and H. D. Politzer, Phys. Rev. Lett. **34**, 43 (1975); A. De Rújula and S. L. Glashow, Phys. Rev. Lett. **34**, 46 (1975).

[2] Charge-conjugate decays are implicitly assumed throughout the paper.

[3] C. P. Shen *et al.* (Belle Collaboration), Phys. Rev. D **86**, 031102(R) (2012).

[4] C. P. Shen *et al.* (Belle Collaboration), Phys. Rev. D **88**, 011102(R) (2013).

[5] N. E. Adam *et al.* (CLEO Collaboration), Phys. Rev. Lett. **94**, 012005 (2005); G. S. Adams *et al.* (CLEO Collaboration), Phys. Rev. D **73**, 012002 (2006).

[6] C. D. Lü, W. Wang and Y. M. Wang, Phys. Rev. D **75**, 094020 (2007).

[7] C. P. Shen *et al.* (Belle Collaboration), Phys. Rev. D **88**, 052019 (2013).

[8] J.-M. Gérard and G. López Castro, Phys. Lett. B **425**, 365 (1998).

[9] V. L. Chernyak and A. R. Zhitnitsky, JETP Lett. **25**, 510 (1977); G. P. Lepage and S. J. Brodsky, Phys. Rev. D **22**, 2157 (1980); S. J. Brodsky and G. P. Lepage, Phys. Rev. D **24**, 2848 (1981).

[10] V. Chernyak, hep-ph/9906387; V. L. Chernyak and A. R. Zhitnitsky, Phys. Rept. **112**, 173 (1984).

[11] V. V. Braguta, A. K. Likhoded, A. V. Luchinsky, Phys. Rev. D **78**, 074032 (2008).